Free and Forced Convective Flow in a Horizontal Channel Embedded in a Porous Medium

Sanatan Das
Department of Mathematics
University of Gour Banga
Malda 732 103, India

Mrinal Jana
Department of Applied Mathematics
Vidyasagar University
Midnapore 721 102, India

Rabindra Nath Jana
Department of Applied Mathematics
Vidyasagar University
Midnapore 721 102, India

ABSTRACT
An exact solution of the governing equations has been obtained for the free and forced convection flow between infinitely long horizontal parallel plates embedded in a porous medium. It is found that the fluid velocity decreases with an increase in porosity parameter. It is also found that the critical Grashof number for which there is no flow reversal near the upper plate decreases with an increase in porosity parameter. Further, the fluid temperature increases with an increase in either porosity of the porous medium or the Grashof number.

Keywords: Free and forced convection, buoyancy force, porous medium and Eckert number.

1. INTRODUCTION
The study of flows through a porous medium is of great importance due to its wide applications in many engineering and technical fields, namely, in Petroleum technology to study the movement of natural gas, oil and water through the oil reservoirs, in the fields of agricultural engineering to study the underground water. The study of convection process in porous media is a well-developed field of investigation because of its important roles and wide applications in thermal insulation, geothermal energy technology, building thermal insulation, heat exchangers, underground disposal of chemical and nuclear waste, coal and grain storage etc. The literature on the topic of free and forced convection in porous medium is well surveyed by Nield and Bejan [1], Bejan [2], Ingham and Pop [3], Kaviany [4] and Kennedy[5]. The study of Combarnous and Bia [6] was one of the first to apply experiments and numerical computation to the effect of mean flow on the onset of convection in a porous medium bounded by isothermal planes. Cheng [7] and Minkowycz et al.[8] conducted a series of studies on mixed convection over vertical, inclined and horizontal plates in porous media. Haajizadeh and Tien [9] have investigated mixed convective flow through a horizontal porous channel that connected two reservoirs. The convection in a porous medium with inclind temperature gradient has been studied by Nield [10]. The combined free and force convective flow in a vertical channel on taking viscous dissipation and pressure work have been studied by Barletta and Nield [11, 12]. Magyari [13] reconsiders the Berletta and Nield's [11] problem and discussed the concept of eigen flow in detail. Fully developed combined free and forced convection flow in a vertical channel bounded by two parallel plates embedded in a porous medium have been studied by Kumar et al. [14].

In the present paper, we have considered the free and forced convective flow between infinitely long horizontal parallel plates embedded in a porous medium. It is found that the fluid velocity increases with an increase in porosity of the porous medium. Further, it is seen that for small values of porosity parameter σ, there is a flow reversal near the upper plate. It is found that the critical Grashof number at the upper plate for which there is no flow reversal near the upper plate decreases with an increase in σ. It is also found that the fluid temperature increases with an increase in porosity parameter σ. Further, the effect of porosity on the fluid temperature is prominent for small values of porosity parameter σ.

2. FORMULATION OF THE PROBLEM AND ITS SOLUTION

We consider the steady viscous incompressible fluid flow through a porous medium between infinitely long horizontal parallel plates. The distance between the two plates is $2L$. Choose a Cartesian co-ordinate system with the x-axis in the direction of the flow and z-axis perpendicular to the plates shown in Fig.1.

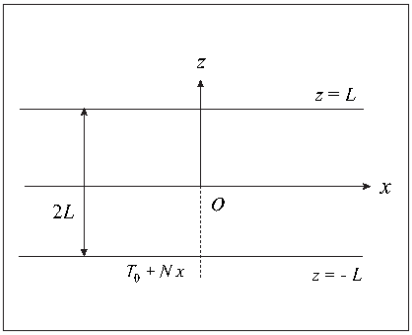

Fig.1. Geometry of the problem

The governing equations for the free and forced convective steady flow through a porous medium on taking Brickmann model can be written as

$$0 = -\frac{\partial p}{\partial x} + \bar{\mu}\frac{\partial^2 u}{\partial z^2} - \frac{\mu}{k^*}u, \quad (1)$$

$$0 = -\frac{\partial p}{\partial z} - \rho g, \quad (2)$$

where u is the fluid velocity, p the fluid pressure, $\bar{\mu}$ the viscosity of the fluid, μ the viscosity of the porous medium, ρ the density of the fluid, k^* the permeability of the porous medium and g the acceleration due to gravity.

The equation of state under the Boussinesq approximation is assumed to be

$$\rho = \rho_0[1-\beta(T-T_0)], \quad (3)$$

where T is the fluid temperature, β the co-efficient of thermal expansion, ρ_0 and T_0 are respectively the density and the temperature in the reference state.

On the use of (3), the equation (2) can be written as

$$0 = -\frac{\partial p}{\partial z} - \rho_0 g[1 - \beta(T - T_0)].$$

(4)

Integrating the equation (4), we get

$$p = -\rho_0 g \int [1 - \beta(T - T_0)]dz + F(x).$$

(5)

In the above equation the integration constant may be an arbitrary function of x, say $F(x)$. Assuming that the wall temperature has a uniform gradient N along the x-direction, the temperature of the fluid can be written as

$$T - T_0 = Nx + \phi(z).$$

(6)

On the use of equations (5) and (6), the equation (1) becomes

$$\nu \frac{d^2u}{dz^2} - \frac{\mu}{\rho_0 k^*} u - g\beta N z = \frac{1}{\rho_0}\frac{dF}{dx},$$

(7)

where $\nu = \frac{\bar{\mu}}{\rho_0}$ is the kinematic viscosity.

The velocity boundary conditions are the no-slip conditions at the inner surface of the wall

$$u = 0 \text{ at } z = \pm L.$$

(8)

Introducing non-dimensional variables

$$\eta = \frac{z}{L}, u_1 = \frac{uL}{\nu},$$

(9)

the equation (7) becomes

$$\frac{d^2u_1}{d\eta^2} - \sigma^2 u_1 - Gr\eta = -P,$$

(10)

where $\sigma^2 = \frac{1}{MDa}$ ($M = \frac{\bar{\mu}}{\mu}$ is the ratio of the viscosities and $Da = \frac{k^*}{L^2}$, the Darcy number) the porosity parameter, $Gr = \frac{g\beta N L^4}{\nu^2}$ the Grashof number and $P = \frac{L^3}{\rho_0 \nu}\left(-\frac{dF}{dx}\right)$. Again, the equation (6) asserts that positive and negative values of N correspond to the heating and the cooling along the channel walls respectively. Evidently, it follows that $Gr >$ or < 0 according as the channel walls are heated or cooled in the axial direction.

The corresponding boundary conditions (8) become

$$u_1 = 0 \text{ at } \eta = \pm 1.$$

(11)

The solution of the equation (10) subject to the boundary conditions (11) is

$$u_1 = \frac{P}{\sigma^2}\left(1 - \frac{\cosh\sigma\eta}{\cosh\sigma}\right) + \frac{Gr}{\sigma^2}\left(\frac{\sinh\sigma\eta}{\sinh\sigma} - \eta\right).$$

(12)

On taking Brickmann model, [see Ingham and Pop [3]] the energy equation is

$$u\frac{\partial}{\partial x}(T - T_0) = \alpha\frac{\partial^2}{\partial z^2}(T - T_0) + \frac{\bar{\mu}}{\rho_0 c_p}\left(\frac{du}{dz}\right)^2 + \frac{\mu}{\rho_0 c_p k^*}u^2 - \frac{\bar{\mu}u}{\rho_0 c_p}\frac{d^2u}{dz^2}, \quad (13)$$

where α is the thermal diffusivity of the fluid and c_p the specific heat. The last two terms in the above equation are due to the porosity of the medium.

On the use of (6) and (9), the equation (13) becomes

$$\frac{d^2\theta}{d\eta^2} = Pru_1 - PrEc\left[\left(\frac{du_1}{d\eta}\right)^2 + \sigma^2 u_1^2 - u_1\frac{d^2u_1}{d\eta^2}\right],$$

(14)

where

$$Pr = \frac{\nu}{\alpha},\ \theta = \frac{\phi}{NL},\ Ec = \frac{\nu^2}{c_p N L^3}.$$

(15)

As for the temperature boundary conditions, we take the reference temperature T_0 such that the temperature at the lower plate $(\eta = -1)$ is $T_0 + Nx$ and this, by virtue of (6), implies $\phi(-1) = 0$. Hence, using (15), the boundary condition for $\theta(\eta)$ are given by

$$\theta(-1) = 0 \text{ and } \theta(1) = \frac{\phi(1)}{NL} = r_T,$$

(16)

where r_T is the plate temperature parameter.

On the use of (12), the equation (14) becomes

$$\begin{aligned}\frac{d^2\theta}{d\eta^2} = Pr\left[\frac{P}{\sigma^2}\left(1 - \frac{\cosh\sigma\eta}{\cosh\sigma}\right) + \frac{Gr}{\sigma^2}\left(\frac{\sinh\sigma\eta}{\sinh\sigma} - \eta\right)\right] \\ -Pr\,Ec\left[a_1 + \frac{P^2}{2\sigma^2}\frac{\cosh 2\sigma\eta}{\cosh^2\sigma}\right. \\ + \frac{Gr^2}{\sigma^4}\left(\frac{\sigma^2\cosh 2\sigma\eta}{2\sinh^2\sigma} - 2\sigma\frac{\cosh\sigma\eta}{\sinh\sigma}\right) \\ - \frac{2PGr}{\sigma^3}\left(\frac{\sigma\sinh 2\sigma\eta}{\sinh 2\sigma} - \frac{\sinh\sigma\eta}{\cosh\sigma}\right) \\ + \frac{P^2}{\sigma^2}\left(1 - \frac{\cosh\sigma\eta}{\cosh\sigma}\right) - \frac{Gr^2}{\sigma^2}\left(\eta\frac{\sinh\sigma\eta}{\sinh\sigma} - \eta^2\right) \\ \left. + \frac{PGr}{\sigma^2}\left(\frac{\sinh\sigma\eta}{\sinh\sigma} + \eta\frac{\cosh\sigma\eta}{\cosh\sigma} - 2\eta\right)\right],\end{aligned}$$

(17)

where

$$a_1 = -\frac{P}{2\sigma^2\cosh^2\sigma} + \frac{Gr^2}{\sigma^4\sinh^2\sigma}\left(\frac{1}{2}\sigma^2 + \sinh^2\sigma\right).$$

(18)

The solution of the equation (17) subject to the boundary conditions (16) is

$$\begin{aligned}\theta(\eta) = \frac{r_T(1+\eta)}{2} + \frac{PPr}{\sigma}\left[\left(\frac{1}{2}\eta^2 - \frac{\cosh\sigma\eta}{\sigma^2\cosh\sigma}\right) - \left(\frac{1}{2} - \frac{1}{\sigma^2}\right)\right] \\ + \frac{PrGr}{\sigma^2}\left[\left(\frac{\sinh\sigma\eta}{\sigma^2\sinh\sigma} - \frac{1}{6}\eta^3\right) - \left(\frac{1}{\sigma^2} - \frac{1}{6}\right)\eta\right] \\ -Pr\,Ec\left[\frac{1}{2}a_1(\eta^2 - 1) + \frac{P^2}{8\sigma^4}\left(\frac{\cosh 2\sigma\eta}{\cosh^2\sigma} - \frac{\cosh 2\sigma}{\cosh^2\sigma}\right)\right. \\ + \frac{Gr^2}{\sigma^4}\left\{\left(\frac{\cosh 2\sigma\eta}{8\sinh^2\sigma} - \frac{2}{\sigma}\frac{\cosh\sigma\eta}{\sinh\sigma}\right) - \left(\frac{\cosh 2\sigma}{8\sinh^2\sigma} - \frac{2}{\sigma}\frac{\cosh\sigma}{\sinh\sigma}\right)\right\} \\ - \frac{2PGr}{\sigma^3}\left\{\left(\frac{\sinh 2\sigma\eta}{4\sigma\sinh 2\sigma} - \frac{\sinh\sigma\eta}{\sigma^2\cosh\sigma}\right) - \eta\left(\frac{1}{4\sigma} - \frac{\sinh\sigma}{\sigma^2\cosh\sigma}\right)\right\} \\ \left. + \frac{P^2}{\sigma^2}\left\{\left(\frac{1}{2}\eta^2 - \frac{\cosh\sigma\eta}{\sigma^2\cosh\sigma}\right) - \left(\frac{1}{2} - \frac{1}{\sigma^2}\right)\right\}\right]\end{aligned}$$

$$+\frac{Gr^2}{\sigma^2}\left\{\frac{1}{12}(\eta^4-1)-\frac{1}{\sigma^2}\left(\frac{\eta\sinh\sigma\eta}{\sinh\sigma}-\frac{2}{\sigma}\frac{\cosh\sigma\eta}{\sinh\sigma}\right)\right.$$
$$\left.+\frac{1}{\sigma^2}\left(1-\frac{2}{\sigma}\frac{\cosh\sigma}{\sinh\sigma}\right)\right\}$$
$$+\frac{PGr}{\sigma^2}\left\{\left[\frac{1}{\sigma^2}\left(\frac{\sinh\sigma\eta}{\sinh\sigma}+\eta\frac{\cosh\sigma\eta}{\cosh\sigma}-\frac{2}{\sigma}\frac{\sinh\sigma\eta}{\cosh\sigma}\right)-\frac{1}{3}\eta^3\right]\right.$$
$$\left.-\left[\frac{1}{\sigma^2}\left(2-\frac{2}{\sigma}\frac{\sinh\sigma}{\cosh\sigma}\right)-\frac{1}{3}\right]\eta\right\}\Bigg].$$

(19)

3. RESULTS AND DISCUSSION

To study the effect of the porosity of the porous medium and the Grashof number on the velocity field, we have plotted the fluid velocity u_1 against η for several values of the porosity parameter σ and Grashof number Gr when $P=1$ in Figs.2 and 3. It seen from Fig.2 that for fixed value of Grashof number Gr, the fluid velocity u_1 decreases with an increase in porosity parameter σ. Fig.3 shows that with an increase in $Gr(Gr>0)$, that is, for heating the fluid velocity u_1 increases in the lower half of the channel while it decreases in the upper half of the channel. The situation is clearly reversed for the negative values of $Gr(Gr<0)$, i.e. for cooling. It is observed that the velocity profiles are asymmetric due to the presence of buoyancy force $Gr(\neq 0)$.

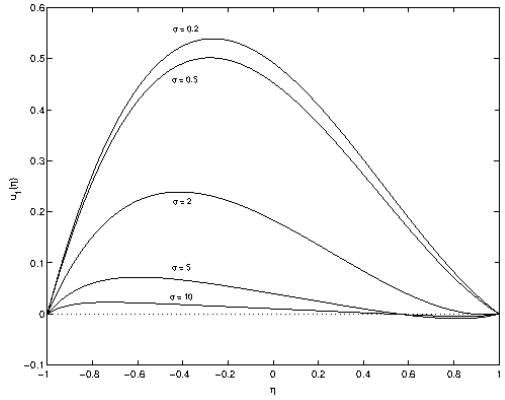

Fig.2: Variations of velocity u_1 for different σ when $Gr=2$.

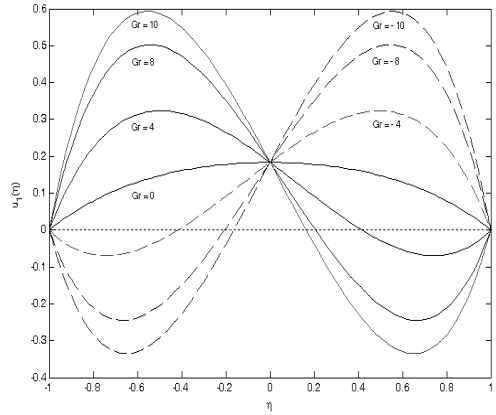

Fig.3: Variations of velocity u_1 for different Gr when $\sigma=0.5$

We consider the following particular cases of interest.

(i) When $\sigma \to 1$, then the velocity field is given by

$$u_1 = P\left[\frac{1}{2}\left(1-\eta^2\right)-\frac{\sigma^2}{24}\left(\eta^4-6\eta^2+5\right)\right]$$
$$+Gr\left[\frac{1}{6}\left(\eta^3-\eta\right)+\frac{\sigma^2}{360}\left(3\eta^5-10\eta^3+7\eta\right)\right]. \qquad (20)$$

Equation (20) shows that the effect of porosity on the fluid velocity is important only when we consider the order $O(\sigma^2)$.

Further, if $\sigma \to 0$ and $Gr \to 0$, then we have

$$u_1 = \frac{P}{2}\left(1-\eta^2\right).$$

(21)

Equation (21) gives the fluid velocity for the hydrodynamic viscous incompressible fluid flow between two infinitely long horizontal parallel plates.

(ii) When $\sigma \to 1$, then the velocity field is given by

$$u_1 = \frac{1}{\sigma^2}\left[\left(P-Gr\eta\right)-\left(P-Gr\right)e^{-\sigma(1-\eta)}\right].$$

(22)

It is seen from the equation (22) that for large values of σ, there exists a thin boundary layer near the vicinity of the upper plate. The thickness of this layer is of order $O(\sigma^{-1})$ which decreases with an increase in porosity parameter σ.

The non-dimensional shear-stress at the plates $\eta=-1$ and $\eta=1$ are respectively given by

$$\tau_0 = \left[\frac{du_1}{d\eta}\right]_{\eta=-1} = \frac{P}{\sigma}\tanh\sigma+\frac{Gr}{\sigma^2}(\sigma\coth\sigma-1), \qquad (23)$$

$$\tau_1 = \left[\frac{du_1}{d\eta}\right]_{\eta=1} = -\frac{P}{\sigma}\tanh\sigma+\frac{Gr}{\sigma^2}(\sigma\coth\sigma-1). \qquad (24)$$

The values of non-dimensional shear stresses at the plates $\eta=-1$ and $\eta=1$ are shown in Figs.4 and 5 respectively for several values of σ and Gr. It is observed from Fig.4 that the shear stress at the lower plate increases with an increase in Gr while it decreases with an increase in σ. On the other hand, Fig.5 shows that for fixed values of σ the shear stress at the upper plate increases with an increase in Gr. Further, the shear stress at the upper plate increases or decreases according to Gr is small or large.

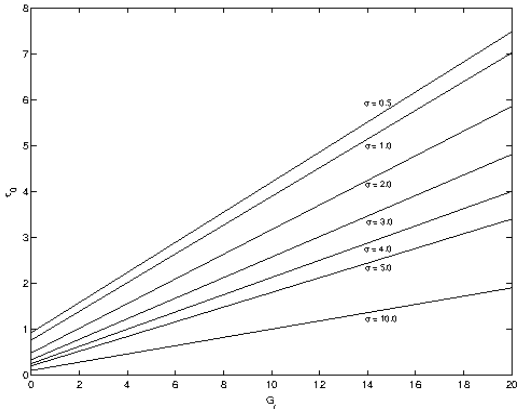

Fig.4: Variations of shear stress τ_0 for against Gr for σ

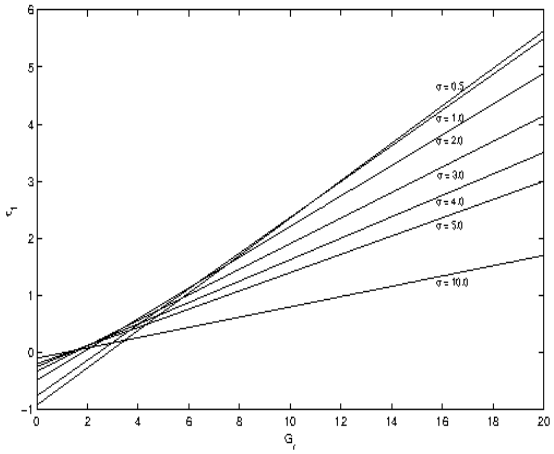

Fig.5: Variations of shear stress τ_1 against Gr for σ

It is seen from the equation (23) that in the absence of buoyancy forces $(Gr = 0)$, the shear stress at the lower plate $\eta = -1$ is always positive. Thus, in this case, there is no flow separation. The shear stress at the lower plate $\eta = -1$ progressively decrease when the lower plate is cooling more and more (which corresponds to negative values of Gr).

The shear stress τ_0 at the lower plate vanishes if

$$(Gr)_{\text{crit}_0} = -\frac{P\sigma \tanh\sigma}{\sigma\coth\sigma - 1}, \tag{25}$$

which leads to occur the incipient flow reversal near the lower plate $\eta = -1$. Further, this leads us to conclude that for fixed value of the porosity of the medium cooling at the lower plate causes tendency towards instability. The cooling of the lower plate gives rise to a component of buoyancy force opposite to the direction of the pressure gradient along the channel which drives the forced convection flow.

The equation (24) shows that the shear stress τ_1 is always negative for cooling $(Gr < 0)$ at the upper plate $\eta = 1$. That is why, there is no flow reversal near the upper plate. However, the shear stress τ_1 at the upper plate vanishes if

$$(Gr)_{\text{crit}_1} = \frac{P\sigma \tanh\sigma}{\sigma\coth\sigma - 1}. \tag{26}$$

This implies that for fixed values of σ, heating of the upper plate $(Gr > 0)$ causes incipient flow reversal there and thus increases the tendency of instability. It is seen from Table 1 that the critical Grashof number $(Gr)_{\text{crit}_1}$ at the upper plate $\eta = 1$ decreases with an increase in porosity parameter σ.

Table 1. critical Grashof number $(Gr)_{\text{crit}_1}$ at the plate $\eta = 1$ when $P = 1$

σ	0.1	0.2	0.5	2	10
$(Gr)_{\text{crit}_1}$	2.99205	1.96853	2.81859	1.79416	1.11111

The fluid temperature distribution have been drawn for several values of σ and Gr when $Pr = 0.71$, $P = 1$, $Ec = 0.5$ and $r_T = 0.5$ in Figs.6 and 7. It is seen from Figs.6 and 7 that the fluid temperature increases with an increase in either Grashof number Gr or porosity parameter σ.

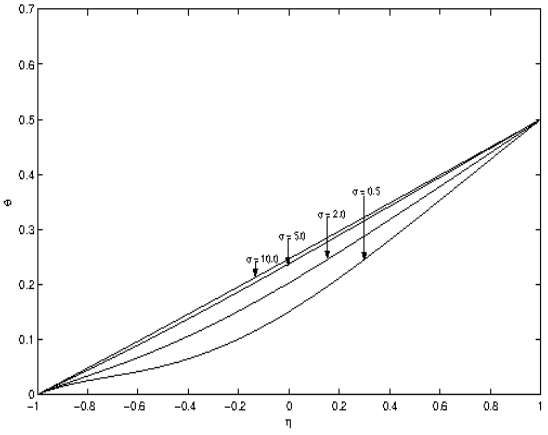

Fig.6: Variations of temperature $\theta(\eta)$ for σ with $Gr = 2$, $Pr = 0.71$, $Ec = 0.5$ and $r_T = 0.5$.

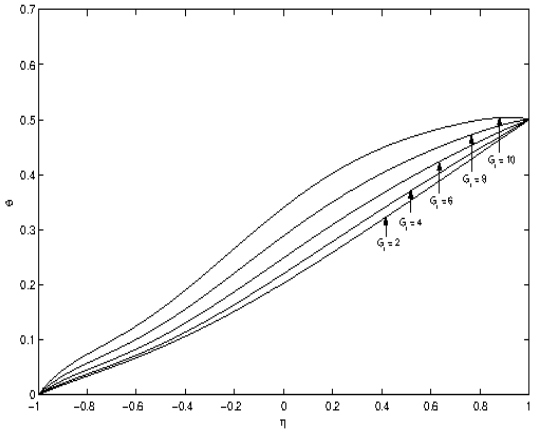

Fig.7. Variations of temperature $\theta(\eta)$ for Gr with $\sigma = 0.5$, $Pr = 0.71$, $Ec = 0.5$ and $r_T = 0.5$.

The rate of heat transfer at the plates $\eta = -1$ and $\eta = 1$ are respectively given by

$$\theta'(-1) = \left[\frac{d\theta}{d\eta}\right]_{\eta=-1} = X_1 - EcPrY_1, \tag{27}$$

$$\theta'(1) = \left[\frac{d\theta}{d\eta}\right]_{\eta=1} = X - EcPrY, \tag{28}$$

where

$$X = \frac{1}{2}r_T + \frac{PPr}{\sigma^3}(\sigma - \tanh\sigma) + \frac{GrPr}{3\sigma^4}\left(3\sigma\coth\sigma - \sigma^2 - 3\right),$$

$$Y = a_1 + \frac{P^2}{2\sigma^3}\tanh\sigma + \frac{Gr^2}{2\sigma^4}(\sigma\coth\sigma - 4)$$
$$- \frac{PGr}{2\sigma^5}\left(2\sigma^2\coth 2\sigma + 4\tanh\sigma - 5\sigma\right)$$
$$+ \frac{P^2}{\sigma^3}(\sigma - \tanh\sigma) - \frac{Gr^2}{3\sigma^4}\left(3\sigma\coth\sigma - \sigma^2 - 3\right)$$
$$+ \frac{PGr}{3\sigma^5}\left\{3\sigma\left(\sigma\coth\sigma + \sigma\tanh\sigma - \sigma^2 - 1\right)\right.$$
$$\left. + \left(6\tanh\sigma + \sigma^3 - 6\sigma\right)\right\},$$

$$X_1 = \frac{1}{2}r_T - \frac{PPr}{\sigma^3}(\sigma - \tanh\sigma) + \frac{GrPr}{3\sigma^4}(3\sigma\coth\sigma - \sigma^2 - 3),$$

$$Y_1 = -a_1 - \frac{P^2}{2\sigma^3}\tanh\sigma + \frac{Gr^2}{\sigma^4}(4-\tanh\sigma) - \frac{PGr}{2\sigma^3}(2\sigma^2\coth 2\sigma + 4\tanh\sigma - 5\sigma) + \frac{P^2}{\sigma^3}(\tanh\sigma - \sigma) + \frac{Gr^2}{3\sigma^4}(3\sigma\coth\sigma - \sigma^2 - 3) + \frac{PGr}{3\sigma^5}\{3\sigma(\sigma\coth\sigma + \sigma\tanh\sigma - \sigma^2 - 1) + (6\tanh\sigma + \sigma^3 - 6\sigma)\}. \quad (29)$$

The rate of heat transfer at the plates $\eta = -1$ and $\eta = 1$ are respectively entered in Tables 2 and 3 for several values of σ and Gr when $P = 1$, $Pr = 0.71$ and $Ec = 0.02$. It is observed from Table 2 that the magnitude of rate of heat transfer at the lower plate $\eta = -1$ first decreases, reaches a minimum and then increases with an increase in porosity parameter σ except for Grashof number $Gr = 0$ while it decreases with an increase in Gr. Table 3 shows that the rate of heat transfer at the upper plate $\eta = 1$ decreases with an increase in either σ or Gr.

Table 2. Rate of heat transfer at the plate $(\eta = -1)$ when $P = 1$

	$\theta'(-1)$				
$Gr \setminus \sigma$	0.2	0.4	0.6	0.8	1.0
0	0.19869	0.18881	0.17416	0.15676	0.13845
4	0.18371	0.17427	0.16122	0.15315	0.17993
8	0.14870	0.13999	0.12908	0.13103	0.23037
12	0.09317	0.08597	0.07773	0.09043	0.20992
16	0.01836	0.01221	0.00718	0.03133	0.19843

Table 3. Rate of heat transfer at the plate $(\eta = 1)$ when $P = 1$

	$\theta'(1)$				
$Gr \setminus \sigma$	0.2	0.4	0.6	0.8	1.0
0	0.47369	0.46381	0.44916	0.43176	0.41345
4	0.46864	0.45860	0.44289	0.41688	0.35433
8	0.44355	0.43366	0.41742	0.38351	0.27755
12	0.39794	0.38897	0.37275	0.33164	0.18312
16	0.33306	0.32454	0.30887	0.26128	0.07104

The critical Eckert number at the plates $\eta = -1$ and $\eta = 1$ for which there is no flow of heat either from plates to fluid or fluid to plates are given by

$$(Ec)_{\text{crit}_1} = \frac{X_1}{PrY_1}, \quad (30)$$

$$(Ec)_{\text{crit}_2} = \frac{X}{PrY}, \quad (31)$$

where X, Y, X_1 and Y_1 are given by (29).

The values of $(Ec)_{\text{crit}_1}$ and $(Ec)_{\text{crit}_2}$ are entered in the Table 4 and 5 for several values of σ and Gr. It is observed from Table 3 that with an increase in Gr the critical Eckert number $(Ec)_{\text{crit}_2}$ at the plate $\eta = -1$ increases for $\sigma \le 0.4$ while it decreases for $\sigma > 0.4$. Further, $(Ec)_{\text{crit}_1}$ decreases with increase in porosity parameter σ when Gr is fixed. Table 5 shows that the critical Eckert number $(Ec)_{\text{crit}_2}$ at the plate $\eta = 1$ decreases with an increase in porosity parameter σ. On the other hand, an increase in Gr leads to increase the critical Eckert number $(Ec)_{\text{crit}_2}$ for $\sigma \le 0.2$ but $\sigma > 0.2$ and decrease first, reaches a minimum and then increases.

Table 4. Critical Eckert number at the plate $(\eta = -1)$ when $P = 1$ and $Pr = 0.71$

	$(Ec)_{\text{crit}_1}$				
$Gr \setminus \sigma$	0.2	0.4	0.6	0.8	1.0
0	1.04484	0.67552	0.24524	0.11364	0.06444
4	1.09482	0.68496	0.24414	0.11334	0.06393
8	1.17800	0.70146	0.24296	0.11193	0.06291
12	1.29418	0.73418	0.23873	0.10619	0.05805
16	1.44305	0.99216	0.23011	0.07794	0.03207

Table 5. Critical Eckert number at the plate $\eta = 1$ when $P = 1$ and $Pr = 0.71$

	$(Ec)_{\text{crit}_2}$				
$Gr \setminus \sigma$	0.2	0.4	0.6	0.8	1.0
0	0.44988	0.17169	0.07021	0.03624	0.02194
4	0.45754	0.17018	0.06867	0.03541	0.02132
8	0.46907	0.16845	0.06703	0.03449	0.02080
12	0.48263	0.17034	0.06995	0.03755	0.02364
16	0.49655	0.18369	0.09308	0.05913	0.04249

It is observed from the equation (28) that the heat will flow from the plate $\eta = 1$ to the fluid if $\left(\frac{d\theta}{d\eta}\right)_{\eta=1} > 0$ which in turn yields, from the equation (31) $(Ec)_{\text{crit}_2} > \frac{X}{PrY}$ while heat will start flowing from the fluid to the plate if $(Ec)_{\text{crit}_2} < \frac{X}{PrY}$. Similarly, the heat flows from the plate $\eta = -1$ to the fluid if $\left(\frac{d\theta}{d\eta}\right)_{\eta=-1} > 0$ which gives, on using (36) $(Ec)_{\text{crit}_1} > \frac{X_1}{PrY_1}$. However, heat starts flowing from the fluid to the plate $\eta = -1$ if $(Ec)_{\text{crit}_1} < \frac{X_1}{PrY_1}$. This reversal of heat flow may be due to the fact that when there is a significant viscous dissipation then the temperature of fluid near plates may exceed the plate temperature. This will cause flow of heat from the fluid to plates even if the plate temperature greater than the fluid temperature. In our heat transfer analysis, we have not only considered the viscous dissipation into account but also taken dissipation due to the porosity of the porous medium. Hence, there is a strong reason for the flow of heat from the fluid to plates under certain conditions.

4. CONCLUSION

The steady free and forced convective flow between two infinitely long horizontal parallel plates embedded in a porous medium has been investigated. It is found that the fluid velocity decreases with an increase in porosity parameter. It is also found that the heating of the upper plate causes flow reversal there while cooling of the lower plate causes flow reversal near the lower plate. It is seen that the rate of heat transfer at the lower plate decreases with an increase in porosity parameter. On the other hand, the rate of heat transfer at the upper plate first decreases, reaches a minimum and then increases with an increase in porosity parameter.

5. REFERENCES

[1] Nield, D. A. and Bejan, A.(1972). Convection in porous media. *New York: Springer, Berlin, Heidelberg*.

[2] Bejan, A.(1994). Convection heat transfer. New York: Weiley.

[3] Ingham, D. B. and Pop, I.(2002). Transport phenomena in porous media-II. *Elsevier science Ltd., The Boulevard, Langford Lane, Kidlington, Oxford OX5, 1GB, UK*.

[4] Kaviany, M.(1995). Principles of heat transfer in porous media. *New York: Springer-Verlay, Inc*.

[5] Kennedy, K. J. and Zebib, A.(1983). Combined free and forced convection between horizontal parallel plates: Some case studies. *Int. J. Heat Mass Transfer*. 26: 471-474

[6] Combarnous, M. A. and Bia, P. (1976). Combined free and forced convection in porous medium. *Soc. Petrol. Eng. J*., 11(7): 399-405.

[7] Cheng, P.(1977). Combined free and forced boundary layer flows about inclined surface in saturated porous media. *Int. J. Heat Mass Transfer*. 20(5): 806-814.

[8] Minkowycz, W. J., Cheng, P. and Hirschberg, R. N.(1984). Non-similar boundary layer analysis of mixed convection about a horizontal heated surface in a fluid-saturated porous medium. *Int. Comm. Heat Mass Transfer*. 11(1): 127-141.

[9] Haajizadeh, M. and Tien, C. L.(1984). Combined nature and forced convection in a horizontal porous channel. *Int. J. Heat Mass Transfer*. 27(6): 799-813.

[10] Nield, D.A.(1998). Convection in a porous medium with inclined termperature gradient amd vertical through flow. *Int. J. Heat Mass Transfer*. 41: 241-243.

[11] Barletta, A. and Nield, D.A.(2009). Combined forced and free convective flow in a vertical porous channel: The effects viscous dissipation and pressure work. *Transp. Porous Med*. 79: 319-334.

[12] Barletta, A. and Nield, D.A.(2009). Comment on Combined forced and free convective flow in a vertical porous channel: The effects of viscous dissipation and pressure work. *Transp.Porous Med*., 80:.389-395.

[13] Magyari, E. (2009). Further Comment on Combined forced and free convective flow in a vertical porous channel: The effects of viscous dissipation and pressure work. *Transp. Porous Med*. 80: 399-400.

[14] Kumar, J. P., Umavathi, J. C., Pop I. and Biradar, B. M. (2009). Fully developed mixed convection flow in a vertical channel containing porous and fluid layer with isothermal or isoflux boundaries. *Transp. porous Med*. 80: 117-135.